

Long-Range Order of the Three-Sublattice Structure in the $S = 1$ Heisenberg Antiferromagnet on a Spatially Anisotropic Triangular Lattice

Hiroki NAKANO¹ *, Synge TODO² †, and Tôru SAKAI^{1,3} ‡

¹Graduate School of Material Science, University of Hyogo, Kouto 3-2-1, Kamigori, Ako-gun, Hyogo 678-1297, Japan

²Institute for Solid State Physics, University of Tokyo, 7-1-26-R501 Port Island South, Kobe 650-0047, Japan

³Japan Atomic Energy Agency, SPring-8, Kouto 1-1-1, Sayo, Hyogo 679-5148, Japan

(Received October 11, 2018)

We study the $S = 1$ Heisenberg antiferromagnet on a spatially anisotropic triangular lattice by the numerical diagonalization method. We examine the stability of the long-range order of a three-sublattice structure observed in the isotropic system between the isotropic case and the case of isolated one-dimensional chains. It is found that the long-range-ordered ground state with this structure exists in the range of $0.7 \lesssim J_2/J_1 \leq 1$, where J_1 is the interaction amplitude along the chains and J_2 is the amplitude of other interactions.

KEYWORDS: Antiferromagnetic Heisenberg spin model, triangular lattice, frustration, spatial anisotropy, numerical diagonalization method, Lanczos method

Frustrated magnets have attracted much attention from the viewpoint of realizing exotic quantum states and phase transitions that occur between such states. One such magnet is the triangular-lattice Heisenberg antiferromagnet. Much effort has been devoted to studies of the $S = 1/2$ model, particularly since Anderson¹ pointed out that this model is a possible candidate for the realization of the spin liquid ground state due to magnetic frustrations. Now, it is widely believed that the ground state of the $S = 1/2$ model has a long-range order (LRO) with a small three-sublattice magnetization.^{2–6} This spin structure is also called the 120 deg structure from the directions of neighboring spins. However, estimating the magnetic order of a three-sublattice structure (3SS) quantitatively by direct methods that are unbiased beyond any approximation or variational method is still difficult even now. Numerical diagonalization data of small finite-size (FS) clusters of up to 36 sites of the $S = 1/2$ model^{5–7} were examined.⁸ However, Leung and Runge⁷ and Bernu *et al.*⁶ reported the subtlety in quantitative extrapolation from their diagonalization data of spin correlation functions for observing the order directly.

Since the LRO occurs as a consequence of the delicate balance of the frustrated situation, the instability of this order is an attractive issue in the case when the model includes factors additional to the triangular-lattice Heisenberg antiferromagnet. One such factor is the spatial anisotropy of interactions in the system. Let us consider that the interaction along a specific direction (J_1) is different from the interaction along the other two directions (J_2) among three equivalent directions in the isotropic case (see Fig. 1); here, we focus our attention on the range of $0 \leq J_2/J_1 \leq 1$. In the case of $J_2 = 0$, the system is reduced to isolated spin chains with an antiferromagnetic interaction, in which the LRO does not occur owing to the one-dimensionality. Therefore, the order

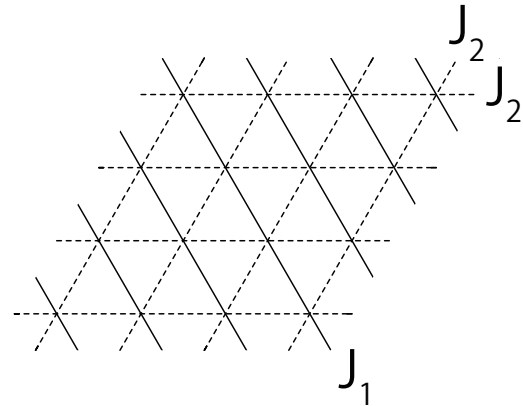


Fig. 1. Spatial anisotropic triangular lattice.

must disappear at a point in this range of $0 \leq J_2/J_1 \leq 1$.

In the classical case of $S = \infty$, the spiral ground state is realized in the range of $0 \leq J_2/J_1 \leq 1$; the behavior is characterized by the canting angle between neighboring spins. In the quantum case, however, not only the canting angle but also sublattice magnetization in the spiral state can be changed due to quantum fluctuation; the situation is different from the classical case. The $S = 1/2$ case has also been tackled.^{11–18} On one hand, there are various reports concerning the range of the spiral state depending on the method.¹⁹ On the other hand, it was shown by the functional renormalization group approach that the LRO in the isotropic case disappears quickly when the anisotropy is switched on.¹⁵ Our understanding of this $S = 1/2$ model has not reached a consensus so far.

In this letter, we examine the $S = 1$ triangular-lattice Heisenberg antiferromagnet with a spatial anisotropy. One major difference of the $S = 1$ case from the $S = 1/2$ case is that the ground state at $J_2 = 0$ in the $S = 1$ case shows the Haldane gap, whereas that in the $S = 1/2$ case is gapless in the spin excitation. It is a nontrivial

*E-mail address: hnakano@sci.u-hyogo.ac.jp

†E-mail address: wistaria@issp.u-tokyo.ac.jp

‡E-mail address: sakai@spring8.or.jp

issue how the existence of the gap affects the magnetically ordered phase, which is supposed to be realized in the isotropic case. Only two approximations^{20,21} have been attempted to elucidate the $S = 1$ case. By a linked-cluster series expansion method,²⁰ it was shown that the ratio J_2/J_1 at the boundary between the magnetically ordered phase of the spiral state and the disordered phase is 0.33. In ref. 21, it was shown by the coupled cluster method that the ordered phase spreads over a range of as low as $J_2/J_1 = 0.25$. In order to obtain an understanding of what beyond any approximation, direct numerical simulations have become increasingly important. However, the quantum Monte Carlo method cannot be applied to the analysis of the triangular-lattice antiferromagnet owing to the so-called negative-sign problem from the frustration in the system. Although the density matrix renormalization method is powerful for the analysis of one-dimensional systems irrespective of whether or not frustration exists, this method is much less effective for the analysis of two-dimensional systems such as a triangular-lattice antiferromagnet. Under these circumstances, the numerically exact diagonalization method based on the Lanczos algorithm is applicable to the triangular-lattice antiferromagnet irrespective of the spatial dimensionality and the existence of magnetic frustration. The purpose of the present study is to extract information on the magnetic LRO from spin correlation functions calculated by the Lanczos diagonalization method in the $S = 1$ FS clusters. The first aim is that the LRO of the three-sublattice structure is quantitatively confirmed in the isotropic case of $J_2 = J_1$ by the direct simulation of Lanczos diagonalization in contrast with the situation mentioned above, for which no such confirmation in the $S = 1/2$ case has been successfully made yet. The further progress in this study clarifies how the LRO behaves in the anisotropic case without having a biased guess based on the argument of the classical system.

Here, we study the Hamiltonian given by

$$\mathcal{H} = J_1 \sum_{\langle i,j \rangle} \mathbf{S}_i \cdot \mathbf{S}_j + J_2 \sum_{[i,j]} \mathbf{S}_i \cdot \mathbf{S}_j, \quad (1)$$

where \mathbf{S}_i denotes the $S = 1$ spin operator. The sum runs over all nearest-neighbor pairs having the antiferromagnetic interaction of J_1 or J_2 . Energies are measured in units of J_1 ; hereafter, we set $J_1 = 1$. The number of spin sites is denoted by N_s . We take $N_s/3$ to be an integer. In all cases of $N_s = 12, 21$, and 27 , we have a rhombic cluster having an interior angle of $\pi/3$, at which the two-dimensionality may be well captured within FS clusters, although only nonrhombic clusters can be formed in the cases of $N_s = 15, 18$, and 24 (see Fig. 2). Note that we exclude the cases in which a system of three-site chains is formed only by J_1 bonds at the point of $J_2 = 0$. We impose the periodic boundary condition for FS clusters. We calculate the lowest energy of \mathcal{H} in the subspace divided by $\sum_j S_j^z = M$. The energy is denoted by $E(N_s, M)$. We also calculate the correlation function $\langle S_i^z S_j^z \rangle$ to observe the LRO.

The weak point of the Lanczos diagonalization method is that only small clusters can be treated owing to the

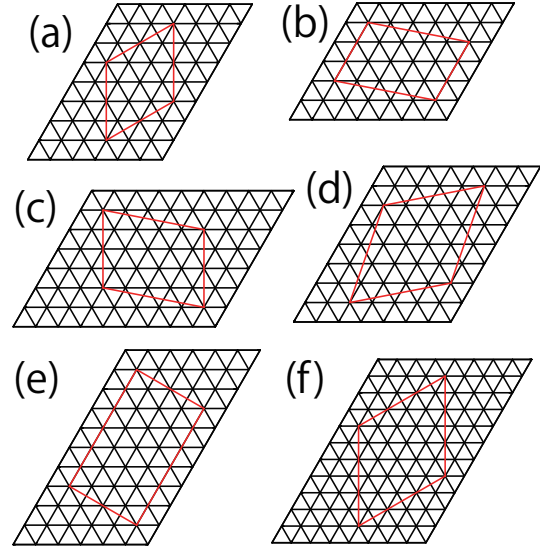


Fig. 2. Shapes of FS clusters of triangular lattice for (a) $N_s = 12$, (b) $N_s = 15$, (c) $N_s = 18$, (d) $N_s = 21$, (e) $N_s = 24$, and (f) $N_s = 27$.

exponential increase in the dimension of the Hamiltonian matrix with respect to the system size. To overcome this problem, we have carried out parallel calculations²² using the MPI-parallelized code²³ to treat system sizes as large as possible. The case of $N_s = 27$ is the largest size in this study.²⁶ In this case, the largest number of dimensions is 712 070 156 203 for the subspace of $M = 0$. Note that this number of dimensions is the largest among those reported in numerical diagonalization studies of quantum lattice systems, to the best of our knowledge.²⁸

Now, we present our results of the $S = 1$ triangular-lattice antiferromagnet for the FS rhombic clusters including the case of $N_s = 27$; these results are listed in Table I. In Fig. 3, the ground-state energy per site $e_g =$

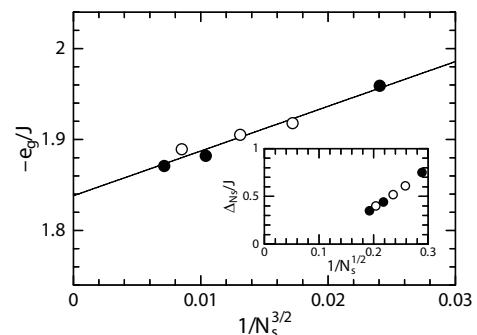


Fig. 3. Ground-state energy per site as a function of $N_s^{3/2}$. In the inset, the $N_s^{1/2}$ dependence of the spin excitation gap is shown. Closed (open) circles represent data for rhombic (nonrhombic) clusters.

$E(N_s, M = 0)/N_s$ is plotted as a function of $N_s^{3/2}$. A linear least-squares fitting gives $-e_g/J_1 = 1.838 \pm 0.007$, which is in agreement with the results of the spin-wave approximation³ and coupled cluster method.²¹ The inset of Fig. 3 depicts the singlet-triplet energy difference

Table I. List of numerical data of the ground-state energy $e_g = E(N_s, M = 0)/N_s$, the singlet-triplet energy difference $\Delta_{N_s} = E(N_s, M = 1) - E(N_s, M = 0)$, and correlation functions for the rhombic clusters. The distance between sites i and j is denoted by $|r_{ij}|$.

N_s	$-e_g/J_1$	Δ_{N_s}/J_1	$\langle S_i^z S_j^z \rangle$				
			$ r_{ij} = 1$	$ r_{ij} = \frac{\sqrt{3}}{2}$	$ r_{ij} = 2$	$ r_{ij} = \sqrt{7}$	$ r_{ij} = 3$
27	1.870821364074	0.348963468544	-0.207869	0.278656	-0.125503	-0.140997	0.253805
21	1.882070035640	0.441247764571	-0.209119	0.286580	-0.138420	-0.150456	
12	1.959106953374	0.751321679528	-0.217679	0.303220	-0.135128		

$\Delta_{N_s} = E(N_s, M = 1) - E(N_s, M = 0)$. The excitation gap seems to vanish in the thermodynamic limit, which is consistent with the existence of the LRO. These results suggest that the FS clusters shown in Fig. 2 are an appropriate series for analyzing our data of correlation functions.

Next, we examine the magnetic order of the triangular-lattice antiferromagnet from FS data of not only rhombic but also nonrhombic clusters. In the isotropic case, let us focus our attention on the signs of $\langle S_i^z S_j^z \rangle$ in Table I. It is possible to group all the spin sites by whether $\langle S_i^z S_j^z \rangle$ is positive or negative so that sites i and j belong to a common group for a positive $\langle S_i^z S_j^z \rangle$. One finds that the grouping divides all the spin sites into three equivalent sublattices. Thus, we evaluate the quantity defined as

$$m_{\text{diag}}^{\text{sq}} = \frac{1}{N_\alpha} \sum_\alpha \frac{1}{N_s} \sum_i \frac{1}{N_s/3 - 1} \sum'_{j \in A_i} \langle \mathbf{S}_i \cdot \mathbf{S}_j \rangle, \quad (2)$$

where $\langle \mathbf{S}_i \cdot \mathbf{S}_j \rangle$ is evaluated by $3\langle S_i^z S_j^z \rangle$, some of which are obtained from the values of spin correlation functions presented in Table I, by taking into account the isotropic interactions in the spin space. Here, the prime at the sum means that j runs over the sublattice A_i including i while excluding the case of $j = i$. Here, α denotes the label of directions concerned which is chosen as J_1 among the three directions; we take the average with respect to the direction in order to take the nonrhombic cases into account. The quantity $m_{\text{diag}}^{\text{sq}}$ corresponds to the squared sublattice magnetization in the thermodynamic limit when the system is magnetically ordered. It is known that, in the isotropic case, the spin-wave approximation³ estimates the sublattice magnetization to be $m_{\text{sw}} = S - \Delta_0 + O[1/S]$ with $\Delta_0 = 0.261$. For $S = 1$, $m_{\text{sw}}^2 = 0.546$, which will be compared with the value extrapolated from our FS $m_{\text{diag}}^{\text{sq}}$ in the isotropic case. Note that the quantity $m_{\text{diag}}^{\text{sq}}$ is the same as eq. (2.11d) in ref. 7. Note also that the analysis of $m_{\text{diag}}^{\text{sq}}$ does not directly provide us with information on the relationship between spins in different sublattices.

We depict $m_{\text{diag}}^{\text{sq}}$ in Fig. 4 as a function of $1/N_s^{1/2}$. One can see oscillating behavior in the system size dependence with respect to whether N_s is odd or even; thus, the data series of odd N_s and even N_s should be treated separately from each other. Note here that each series of $m_{\text{diag}}^{\text{sq}}$ should converge to a common value in the thermodynamic limit. Then, we perform a linear least-squares fitting to each series under the constraint condition of a common intercept. From the analysis without $N_s = 27$, we obtain the fitting lines in Fig. 4, drawn as the solid line for the data of $N_s = 12, 18,$ and 24 and as the dot-

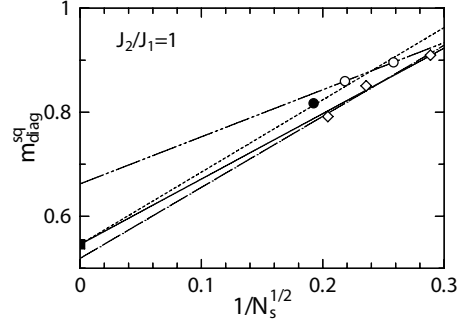


Fig. 4. Extrapolation analysis of FS results for $m_{\text{diag}}^{\text{sq}}$ in the isotropic case. Open diamonds denote the results for $N_s = 12, 18,$ and 24 . Open circles represent the results for $N_s = 15$ and 21 . The closed circle represents that for $N_s = 27$, which is the largest system in this study. The result of the spin-wave approximation is plotted by the closed square at the ordinate. See text regarding linear lines.

ted line for the data of $N_s = 15$ and 21 . The common intercept is obtained to be

$$0.546 \pm 0.051, \quad (3)$$

as an extrapolated value. From the analysis with $N_s = 27$, we have the common intercept

$$0.551 \pm 0.035, \quad (4)$$

which is in agreement with the result (3). Note that both results (3) and (4) are in agreement with the spin-wave result mentioned above. Therefore, the constraint-condition analysis can provide us with a reliable value from extrapolation even without $N_s = 27$. In Fig. 4, the single-dotted and double-dotted chain lines are also drawn for even N_s and odd N_s , respectively, as simple linear least-squares fittings without considering the constraint condition. One finds that the intercept for even N_s underestimates and that for odd N_s overestimates the squared sublattice magnetization with which the result of the constraint-condition analysis is in agreement.

Next, we examine the anisotropic case of $J_2/J_1 < 1$; the FS result of $m_{\text{diag}}^{\text{sq}}$ for each N_s as a function of J_2/J_1 is shown in Fig. 5. One can observe that the magnetic order decreases rapidly as J_2/J_1 is decreased. We perform the constraint-condition analysis in the cases of $J_2/J_1 = 0.5$ and 0.8 ; the analysis for extrapolation is shown in Fig. 6. The common intercept was obtained to be 0.04 ± 0.17 for $J_2/J_1 = 0.5$, which indicates that the LRO of the 3SS disappears. On the other hand, we obtain a positive common intercept for $J_2/J_1 = 0.8$; the result of $J_2/J_1 = 0.8$ is shown in Fig. 5 together with the result in the case

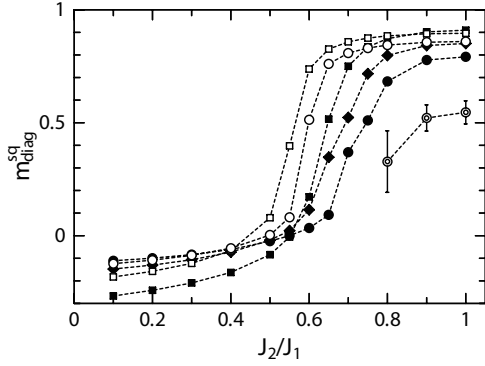


Fig. 5. FS results for $m_{\text{diag}}^{\text{sq}}$. Closed squares, diamonds, and circles denote the results for $N_s = 12, 18,$ and 24 , respectively. Open squares and circles represent the results for $N_s = 15$ and 21 , respectively. Double circles with the error bar denote extrapolated results from the constraint-condition analysis of data up to $N_s = 24$ for $J_2/J_1 = 0.8, 0.9,$ and 1 .

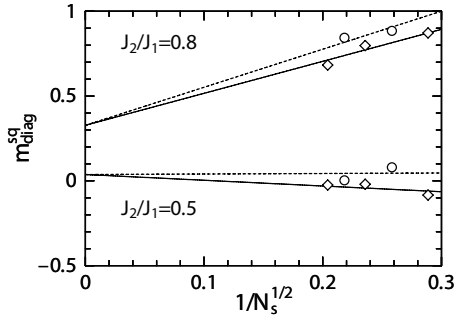


Fig. 6. Extrapolation analysis of FS results for $m_{\text{diag}}^{\text{sq}}$ in the anisotropic cases of $J_2/J_1 = 0.5$ and 0.8 . The procedure of the extrapolation is the same as that in Fig. 4.

of $J_2/J_1 = 0.9$ and the result (3) of $J_2/J_1 = 1$. These results suggest that the LRO of the 3SS survives in a range having a nonzero width.

Between $J_2/J_1 = 0.5$ and 0.8 , unfortunately, the constraint-condition analysis gives a quite large error or a negative common intercept owing to a severe FS effect; it is not so easy to estimate the critical value of J_2/J_1 between the region where the LRO of the 3SS survives and the region where it disappears. In the analysis of only even N_s shown in Fig. 7(a), the intercept at the ordinate changes its sign between $J_2/J_1 = 0.75$ and 0.8 . From the observation of the isotropic case in Fig. 4, J_2/J_1 at the vanishing intercept is considered to be overestimated as the critical value of J_2/J_1 from the result in Fig. 7(a). On the other hand, the analysis of odd N_s shown in Fig. 7(b) indicates that the intercept at the ordinate changes its sign between $J_2/J_1 = 0.6$ and 0.65 ; J_2/J_1 at the vanishing intercept is considered to be underestimated as the critical value of J_2/J_1 from the result in Fig. 7(b). Therefore, it is reasonable to consider that J_2/J_1 at the boundary is 0.7 ± 0.1 .

In summary, we studied the ground state of an $S = 1$ Heisenberg antiferromagnet on a triangular lattice with spatial anisotropy by Lanczos diagonalization calculations with large-scale parallelization; the stability of the

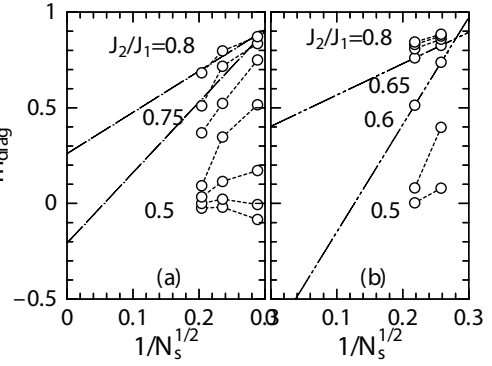


Fig. 7. Extrapolation analysis for $m_{\text{diag}}^{\text{sq}}$ without the constraint condition in the anisotropic cases between $J_2/J_1 = 0.8$ and 0.5 with 0.05 intervals for (a) even- N_s results and (b) odd- N_s results.

long-range magnetic order of the 3SS is examined. We found that in the isotropic case, our Lanczos diagonalization data of spin correlation functions are successfully extrapolated to a long-range-ordered value which is quantitatively consistent with the spin-wave approximation. In the present study, we concluded that, in the range of $0.7 \lesssim J_2/J_1 \leq 1$, the sublattice magnetization gradually shrinks as J_2 is decreased, while the ground state maintains the 3SS. The width of this region is narrower than those of the magnetically ordered state obtained in studies by approximation.^{20,21} In future studies concerning this model, the magnetic structure factor as a function of wave number should be examined in the range near $J_2/J_1 = 1$, which will contribute much to our understanding of the relationship between the spiral states and the states with the LRO of the 3SS obtained in the present study. In the region near $J_2 = 0$ at which the Haldane gap exists, on the other hand, the behavior of the spin excitation gap should also be tackled. Since clusters up to $N_s = 24$ take various tilting angles, it is difficult to observe systematic behavior of the N_s dependence; calculations of the $N_s = 27$ system with anisotropy are required. NiGaS²⁹ and Ba₃NiSb₂O₉³⁰ are considered to be good candidate materials for the $S = 1$ Heisenberg antiferromagnet on the isotropic triangular lattice, although experimental observations and theoretical predictions are not necessarily in agreement with each other in every aspect. Candidate $S = 1$ materials in anisotropic cases would also contribute much to our understanding of magnetic phenomena due to frustration.

Acknowledgments

We wish to thank Professor S. Miyashita, Professor Y. Hasegawa, and Dr. T. Okubo for fruitful discussions. This work was partly supported by Grants-in-Aid (Nos. 23340109, 23540388, and 24540348) from the Ministry of Education, Culture, Sports, Science and Technology of Japan. Some of the computations were performed using facilities of the Department of Simulation Science, National Institute for Fusion Science; Research Institute for Information Technology, Kyushu University; Center for Computational Materials Science, Institute for Materials Research, Tohoku University; The Supercomputer

Center, Institute for Solid State Physics, The University of Tokyo; and Supercomputing Division, Information Technology Center, The University of Tokyo. Our computations in the largest case were carried out with the computational resource of Fujitsu FX10 awarded by the “Large-scale HPC Challenge” Project, Information Technology Center, The University of Tokyo. This work was partly supported by the Strategic Programs for Innovative Research, MEXT, and the Computational Materials Science Initiative, Japan. The authors would like to express their sincere thanks to the crew of Center for Computational Materials Science of the Institute for Materials Research, Tohoku University for their continuous support of the SR16000 supercomputing facilities.

- 1) P. W. Anderson: *Mater. Res. Bull.* **8** (1973) 153.
- 2) D. A. Huse and V. Elser: *Phys. Rev. Lett.* **60** (1988) 2531.
- 3) Th. Jolicour and J. C. Le Guillou: *Phys. Rev. B* **40** (1989) 2727(R).
- 4) R. R. P. Singh and D. A. Huse: *Phys. Rev. Lett.* **68** (1992) 1766.
- 5) B. Bernu, C. Lhuillier, and L. Pierre: *Phys. Rev. Lett.* **69** (1992) 2590.
- 6) B. Bernu, P. Lecheminant, C. Lhuillier, and L. Pierre: *Phys. Rev. B* **50** (1994) 10048.
- 7) P. W. Leung and K. J. Runge: *Phys. Rev. B* **47** (1993) 5861.
- 8) Recently, a 39-site system of an $S = 1/2$ triangular-lattice antiferromagnet was treated in Lanczos diagonalization studies in refs. 9 and 10.
- 9) J. Richter, J. Schulenburg, and A. Honecker: *Lecture Notes in Physics* (Springer-Verlag Berlin Heidelberg, 2004) vol. **645** p. 85.
- 10) T. Sakai and H. Nakano: *Phys. Rev. B* **83** (2011) 100405(R).
- 11) W. Zheng, R. H. McKenzie, and R. P. Singh: *Phys. Rev. B* **59** (1994) 14367.
- 12) S. Yunoki and S. Söllera: *Phys. Rev. B* **74** (2006) 014408.
- 13) O. A. Starykh and L. Balents: *Phys. Rev. Lett.* **98** (2007) 077205.
- 14) D. Heidarian, S. Söllera, and F. Becca: *Phys. Rev. B* **80** (2009) 012404.
- 15) J. Reuther and R. Thomale: *Phys. Rev. B* **83** (2011) 024402.
- 16) A. Weichselbaum and S. R. White: *Phys. Rev. B* **84** (2011) 245130.
- 17) S. Ghamari, C. Kallin, S. S. Lee, and E. S. Sørensen: *Phys. Rev. B* **84** (2011) 174415.
- 18) K. Harada: *Phys. Rev. B* **86** (2012) 184421.
- 19) The reported results are in the range down to $J_2/J_1 \sim 0.85$ obtained by a variational Monte Carlo method,¹⁴ the whole range down to $J_2/J_1 \sim 0$ obtained by a series expansion method,¹¹ and the range down to $J_2/J_1 \sim 0.7$ obtained using a multiscale entanglement renormalization ansatz.¹⁸
- 20) T. Pardini and R. R. P. Singh: *Phys. Rev. B* **77** (2008) 214433.
- 21) P. H. Y. Li and R. F. Bishop: *Eur. Phys. J.* **85** (2012) 25.
- 22) The case of the largest dimension, namely, $N_s = 27$ and $M = 0$, took approximately 167 s per Lanczos step in an MPI-parallelized job with 59 049 processes in the Fujitsu FX10, ITC, The University of Tokyo.
- 23) This parallel code was developed originally in the studies described in refs. 24 and 25.
- 24) H. Nakano and A. Terai: *J. Phys. Soc. Jpn.* **78** (2009) 014003.
- 25) H. Nakano and T. Sakai: *J. Phys. Soc. Jpn.* **80** (2011) 053704.
- 26) In the $S = 1$ case, the maximum size treated in the Lanczos diagonalization method in the previous studies was $N_s = 24$ in ref. 24 to the best of our knowledge, with the criterion of whether the largest subspace with $M = 0$ was treated. Reference 27 reported the $N_s = 27$ case; but only smaller subspaces with a large M were treated.
- 27) J. Richter, O. Götze, R. Zinke, D. J. J. Farnell, and H. Tanaka: *J. Phys. Soc. Jpn.* **82** (2013) 015002.
- 28) The record before the present study was 538 257 874 440 in the study of the $S = 1/2$ kagome-lattice Heisenberg antiferromagnet in ref. 25.
- 29) S. Nakatsuji, Y. Nambu, H. Tonomura, O. Sakai, S. Jonas, C. Broholm, H. Tsunetsugu, Y. Qiu, and Y. Maeno: *Science* **309** (2005) 1697.
- 30) Y. Shirata, H. Tanaka, T. Ono, A. Matsuo, K. Kindo, and H. Nakano: *J. Phys. Soc. Jpn.* **80** (2011) 093702.